Hydrodynamic diffusive behavior of fine particle assemblage passing through nonuniform granular porous media

Ryoko Otomo[a]*, Yuki Nakano[a] and Shusaku Harada[b]

[a]*Department of Mechanical Engineering, Kansai University, Suita, Japan;* [b] *Division of Sustainable Resources Engineering, Hokkaido University, Sapporo, Japan*

otomo@kansai-u.ac.jp

Hydrodynamic diffusive behavior of fine particle assemblage passing through nonuniform granular porous media

We numerically investigated how fine particle assemblages move through pore space of granular media filled with fluid on the assumption of extremely small Reynolds number and Stokes number. We calculated the particle trajectories passing through granular bed with uniform and nonuniform structures by the Stokesian dynamics method, which can take into account hydrodynamic interactions between particles. It was observed that the particle assemblage was moving complexly while avoiding granular bed, resulting in hydrodynamic diffusion. The hydrodynamic diffusive behavior in the traveling and lateral directions was evaluated using the index D_h, which means the particles dispersion increases per unit time. By comparison with the uniform granular bed, it was found that the hydrodynamically-diffusive behavior in the nonuniform bed was quite distinctive. Particularly, in the lateral direction, the particle assemblages showed both positive and negative spreading depending on the non-uniformity. The present results indicate that the relationship between a nonuniform structure and the index D_h could be applied to various engineering processes such as separating and sorting fine particles.

Keywords: Fine particles; Hydrodynamic diffusion; Granular porous media; Nonuniform structure; Stokes flow; Micro-scale transport

1. Introduction

Hindered transport phenomena of fine particles in granular porous media filled with fluid are found in many fields, such as natural fields, chemical engineering, and bioengineering. For example, microscopic transport properties play a significant role in a number of separation and filtration processes (Skaug et al., 2015) and macromolecule transfer in-vivo (Ando and Skolnick, 2010). In recent years, the collaboration between medical science and engineering has been remarkably advanced in the field of biotechnology, and various experiments and analyses on biological cells and microorganisms have been conducted. Since chemical analysis using granular porous

media such as chromatography and biological cell manipulation for separation and collection are essential, micro- and nano-scale flow and transport phenomena are attracting more and more attention. It is crucially important to understand the hindered behavior of substances in porous media and to evaluate its characteristics.

Focusing on transport phenomena of micro-substances in a fluid, the Reynolds number is often very small. Because the fluid viscosity is dominant when *Re* is small, fluid-mediated interaction (hydrodynamic interaction) is generated between substances. In such a system, since the effect of inertia of the substances as well as the fluid is often small, the effect of hydrodynamic interaction is relatively very important. For example, it has been reported that the motion of fine particle assemblages in liquids at $Re << 1$ is very complicated (Crowley, 1971; Ganatos et al., 1978). One of the major factors of the complexity is their long-range character of the hydrodynamic interactions. The hydrodynamic interaction between fine particles is determined by their size and positional relationship. Specifically, the magnitude of the interaction of pairwise particles is proportional to the reciprocal of their distance. Therefore, the prediction of the behavior of fine particles dispersed in a liquid must be carried out taking into account the existence of all particles including distant ones.

When fine particles move collectively in a fluid under the condition of $Re << 1$, diffusion occurs not only due to thermal motion of molecules but also due to hydrodynamic interactions between them. This is called hydrodynamic diffusion (Davis, 1996; Guazzelli and Hinch, 2011). Molecular diffusion is caused by the concentration gradient of a substance, and the diffusion coefficient is the physical property value determined by the combination of a substance and a fluid. In contrast, the hydrodynamic diffusion is difficult to be evaluated, especially in the low Reynolds number condition, due to the long-range hydrodynamic interaction. In the previous studies, hydrodynamic

diffusion in sedimentation of fine particles has been studied by experimentally and numerically, and characteristics such as volume fraction dependence and anisotropy of spreading behavior have been revealed (Nicolai et al., 1995; Guazzelli and Hinch, 2011). The authors conducted a numerical analysis of the particle behavior based on theoretical calculations to examine the hydrodynamic diffusion of a particle layer moving in a quiescent fluid (Harada and Otomo, 2009). As a result, it was found that the slight difference in the initial arrangement of particles had a great influence on the hydrodynamic diffusive behavior.

Hydrodynamic diffusive behavior of fine particle assemblage should occur not only in unobstructed fluid but also in pore fluid in granular porous media mentioned at the beginning of this paper. In this case, the hydrodynamic interaction between fine particles and granular media as well as between fine particles should be taken into account, which makes the phenomenon more complicated. In addition, the granular media does not necessarily have a uniform structure, but there is more or less local porosity difference inside. There have been few examples for detailed analyses of the effect of pore-scale nonuniformity of granular porous media on microscopic behavior of fine particles due to hydrodynamic interactions.

In this study, we numerically investigated how fine particle assemblages move through pore space of granular media filled with fluid on the assumption of micro-scale phenomena with extremely small Reynolds number and Stokes number. Similar to authors' previous studies, the Stokesian dynamics method (Durlofsky et al., 1987; Brady et al., 1988; Brady and Bossis, 1988), which can take into account hydrodynamic interactions between particles, was applied to the calculation of particle behavior. Focusing on the hydrodynamic diffusion, the behavior of fine particles in the traveling direction and in the plane perpendicular to it was investigated in detail by setting an

cylindrical calculation domain. The purpose of this study is to confirm the characteristics of hydrodynamic diffusion different from molecular diffusion, and to quantitatively clarify the effects of volume fraction and nonuniform structure of the granular media on it.

2. Numerical method

2.1 Calculation conditions

2.1.1 Uniform granular bed

Schematic diagram of the computational domain is shown in Fig. 1(a). A cylindrical computational domain is set in a part of the fluid-filled region, in which spherical particles (blue particles) of radius a_s are randomly arranged and fixed to form a granular bed. There are no walls at the boundary of the granular bed (shown by the dotted line in Fig. 1). The pores of granular bed and outside of the computational domain are all filled with same fluid, corresponding to free inflow and outflow boundary conditions.

In this paper, the computational domain was set to a cylindrical shape rather than a rectangular. This is because the length from the center of the domain to the boundary of the side was kept constant, so that the effect of the boundary (end effect) would not be as complicated as possible, when examining the movement of fine particles in the plane perpendicular to the traveling direction (that is called 'radial' or 'lateral' direction hereafter).

The radius and the length of the granular bed region were determined to be $r_{xy} = 15a_s$ and $l_z = 60a_s$, respectively. For the volume fraction of the granular bed ϕ_{uni}, 6 conditions (2%, 3%, 5%, 7%, 10%, and 12%) were adopted, as shown in Fig. 2(a). Since the arrangement of granular beds and initial fine particles (explained in section 2.1.3) was given by random numbers, 15 trials were carried out by changing them.

2.1.2 Nonuniform granular bed

As shown in Fig. 1(b), a "sparse area" with a small volume fraction was set in the middle part of the randomly arranged granular bed, as a system where the volume fraction is different only in a part of the granular bed. The volume fraction of a sparse region is expressed as ϕ_{in}, and the surrounding region is expressed as "dense region" and its volume fraction is expressed as ϕ_{out}. Under this condition, the boundary surface between the sparse and dense regions is parallel to the traveling direction of fine particles. We focus on the lateral behavior of fine particles that across the sparse-dense boundary and how the particle motion in hydrodynamic diffusion is affected by the nonuniformity, while fine particles move in the reverse direction of the concentration gradient in the case of the molecular diffusion. By setting the sparse-dense region in a coaxial cylindrical system, the lateral spread can be expressed not by two components in the x and y directions, but by one component in the radial direction. In addition, as in section 2.1.1, there is an intention not to complicate the end effect on the particle behavior as much as possible.

In this study, as shown in Fig. 2(b), we basically set the dense region as $\phi_{out} =$ 12%, and the sparse regions as 5 conditions, $\phi_{in} =$ 0%, 2%, 5%, 7%, and 12%. The condition $\phi_{in} = 0.12$ is the same as that of a uniform granular bed. The sparse region is within the range of radius $r_{xy,in} = 5.0a_s$ in the x–y plane. The arrangement of granular beds and initial fine particles (explained in section 2.1.3) was changed by the random number, and ten trials were carried out. The other conditions are the same as section 2.1.1.

2.1.3 Fine particles moving through granular bed

Initial arrangement of the fine particle assemblage is shown in Fig. 1. Forty particles of

radius a_m (red particles) are randomly placed in a cylindrical region of height 10 a_s and diameter 15 a_s at the top of the granular bed. For nonuniform granular bed conditions, the number of particles placed in the sparse and dense regions are given according to the respective areas. In the present calculation, 18 and 22 particles were placed in the sparse and dense regions, respectively.

The particles move in the granular bed by external force $F/6\pi\mu a_m U_0 = (0, 0, -1)$. The velocity of each fine particle was calculated by the Stokesian dynamics method shown in the following section. Using the second-order Runge-Kutta method, the particle position up to 10000 steps was obtained as a dimensionless time step $\Delta t/(a_s/U_0) = 0.01$. The initial time when the calculation is started is called the permeation start time (t_{01}=0), and the time when a fine particle in the front reaches out of the region of the granular bed is called the permeation end time (t_{01}=1).

The particle radius ratio of fine particles to fixed particles (forming a granular bed) was set to be $\lambda = a_m / a_s = 0.5$. In the present study, since the main focus is on the non-uniformity of the granular bed, only one condition $\lambda = 0.5$ was adopted. This λ is determined based on authors' preliminary calculations at $\lambda = 0.2$, 0.5 and 1.0, and the previous work at $\lambda = 1.0$ and 2.0 (Otomo and Kira, 2021). In the former preliminary calculations, we have performed simulations similar to the present study. In the latter work, the hydrodynamic diffusive behavior of fine particles through fibrous bed was simulated at the diameter ratio of particles to fibers $\lambda = 1.0$ and 2.0. Within these range of λ, it is indicated that the particle size affects the hydrodynamic diffusive behavior (only the spreading in the traveling direction is evaluated), but the difference is within a few times. Although the effects of the particle size with a few orders of magnitude, the particle polydispersity, and the volume fraction of the moving particles might be also possible, they have not been considered at the present time.

2.2 Stokesian dynamics

The Stokesian dynamics method that enables to calculate the particle motion considering the hydrodynamic interaction was used (Durlofsky et al., 1987; Brady et al., 1988; Brady and Bossis, 1988). Assuming $Re \ll 1$ and $St \ll 1$, the Stokes equations and continuity equations for incompressible fluids with viscosity μ were used as the basic equations. By multipole expansion of the fluid velocity $\boldsymbol{u}$ obtained as the solution of the basic equations in the presence of particles, the following equation can be obtained as the flow field at any position $\boldsymbol{x}$,

$$v_i(\boldsymbol{x}) = u_i^{\infty}(\boldsymbol{x}) + \frac{1}{8\pi\mu}\sum_{\beta=1}^{N}\left[\left(1+\frac{1}{6}a_\beta^2\nabla^2\right)J_{ij}\left(\boldsymbol{x}-\boldsymbol{x}^\beta\right)F_j^\beta + R_{ij}\left(\boldsymbol{x}-\boldsymbol{x}^\beta\right)T_j^\beta + \cdots\right] \qquad (1)$$

where u_i^{∞} is the flow field in the absence of particles, a^β is the radius of particle β, $\boldsymbol{x}^\beta$ is the center position of particle β, and F_j^β and T_j^β are the force and torque, respectively, acting on the fluid from particle β. The equations $J_{ij}(\boldsymbol{r}) = \delta_{ij}/r + r_i r_j / r^3$ and $R_{ij}(\boldsymbol{r}) = -e_{ijk}r_k / r^3$ play a role in weighting the effects of the force and torque, respectively, on the flow field at any position $\boldsymbol{x}$ by the distance from the particle (r is the distance from the particle center, $\boldsymbol{r} = \boldsymbol{x} - \boldsymbol{x}^\beta$). On the other hand, if a particle α is placed in a flow field $\boldsymbol{v}(\boldsymbol{x})$, the fluid force $\boldsymbol{F}^{\mathrm{f}}$ acting on the particle α is expressed as follows (Faxén's law):

$$F_i^{\mathrm{f}} = 6\pi\mu a_\alpha\left(1+\frac{1}{6}a_\alpha^2\nabla^2\right)v_i\left(\boldsymbol{x}^\alpha\right) - 6\pi\mu a_\alpha U_i^\alpha \qquad (2)$$

where $\boldsymbol{x}^\alpha$ and $\boldsymbol{U}^\alpha$ represent a center coordinate and velocity of particle α, respectively (Kim and Karrila, 2005). a_α is the radius of particle α. The fluid force $\boldsymbol{F}^{\mathrm{f}}$ has an action-reaction relationship with the force $\boldsymbol{F}^\alpha$ acting from the particle α to the fluid. By combining Eqs. 1 and 2, the velocity of each particle can be determined, taking into account the hydrodynamic effects of the presence of all particles. When the inertia of

particles and fluid is negligibly small, the relation between the relative velocity $\boldsymbol{U}-\boldsymbol{u}^{\infty}$ of particles and fluid and the external force $\boldsymbol{F}$ acting on each particle is expressed,

$$\boldsymbol{U}-\boldsymbol{u}^{\infty}=\boldsymbol{M}\cdot\boldsymbol{F} \tag{3}$$

where $\boldsymbol{M}$ is the mobility matrix determined by the position relation of each particle. Since only the translational motion of particles was treated in this study, the F-version, which takes into account up to the force term of the infinite series in Eq. 1, was adopted (Phillips et al., 1988). The mobility matrix in the F-version is represented as follows:

$$M_{ij}(\boldsymbol{r})=\begin{cases}\delta_{ij} & (\alpha=\beta)\\ \left(\frac{3}{4}a_{\alpha}+\frac{1}{8}a_{\alpha}\left(a_{\alpha}^{2}+a_{\beta}^{2}\right)\nabla^{2}\right)\left(\nabla^{2}\delta_{ij}-\nabla_{i}\nabla_{j}\right)r & (\alpha\neq\beta)\end{cases} \tag{4}$$

The correction of the lubrication effect between particles was carried out by the Jeffrey and Onishi (1984) method where the mobility matrix is corrected by exact solution of the interaction of all two-particle combinations.

In the presence of particles (stationary particles) fixed in space, the velocity of particles (mobile particles) moving through the stationary particles is expressed based on Eq. 3 (Nott and Brady, 1994; Singh and Nott, 2000),

$$\boldsymbol{U}^{\mathrm{M}}=\boldsymbol{u}^{\infty}+\left(\boldsymbol{R}^{\mathrm{MM}}\right)^{-1}\cdot\left(\boldsymbol{F}^{\mathrm{M}}-\boldsymbol{R}^{\mathrm{MS}}\cdot\boldsymbol{U}^{\mathrm{S}}+\boldsymbol{R}^{\mathrm{MS}}\cdot\boldsymbol{u}^{\infty}\right) \tag{5}$$

where the superscripts S and M are the stationary and mobile particles, respectively, and $\boldsymbol{R}$ is the inverse matrix of the mobility matrix $\boldsymbol{M}$, and the relation between each kind of particles was extracted. Since the velocity of the stationary particle is zero, the velocity of the mobile particle was calculated from the flow field in the absence of particles and the external force acting on it.

As a verification of the validity of the present method, it has been confirmed in our previous study that the behavior satisfying reversibility, which is a characteristic of Stokes flow, can be obtained when the translational motion of the fine particle layer in liquid was calculated (Harada and Otomo, 2009). In addition, the trajectory of fine mobile particle translating around particles fixed in the stationary fluid was calculated. As a result, the behavior which satisfies the symmetry which is also the characteristic of Stokes flow was obtained (Otomo and Mori, 2021).

2.3 Repulsive force between particles to avoid overlapping

In this study, numerical errors due to the calculation method and to the time evolution were generated, and consequently particles sometimes overlapped each other. In order to prevent the overlap, the repulsive force between particles, examined by Nott and Brady (1994), and Singh and Nott (2000), was taken into account. The repulsive force which acts among all particles is given by the following equation,

$$F_{\mathrm{rep}} = \frac{\tau \exp\left(-\tau D\right)}{1-\exp\left(-\tau D\right)} \tag{6}$$

where D is the distance between particle surfaces. The values $F_0 = 0.001$ and $\tau = 1000$ were set based on the Nott and Brady (1994), and Singh and Nott (2000). The relationship between the surface distance of two particles and the magnitude of repulsive force is shown in Fig. 3. When the distance between particle surfaces is very small, the repulsive force acts greatly, but when the distance is large, the repulsive force becomes almost zero. Therefore, the repulsive force shown in Eq. 6 enables to prevent the particle overlap without affecting the behavior of particles. This repulsive force is a numerical force, and has no physical meaning.

3. Results and Discussions

3.1 Behavior of fine particle assemblage through uniform bed

Figure 4 shows an example of calculation results of fine particle assemblage behavior moving in a stationary granular bed with various volume fractions. For the better understanding for the fine particle position, the particle bed is represented in translucent. From Fig. 4, it is understood that the fine particle assemblage permeates the granular bed while changing the relative position by hydrodynamic interaction. Under the conditions of $Re < 1$ and $St < 1$, it is known that the collision between fine particles or between fine particle and granular bed does not occur because the inertia of the fluid and particles is small ($St < 10$, presented by Joseph et al., 2001). In the present results, such collisions were not observed, and it was confirmed that fine particles were permeating while moving in a complicated lateral direction as if they avoided granular bed.

Comparing the fine particle positions at the time of the beginning and the end of permeation, it can be seen that the fine particle assemblages spread widely. This is a result of the hydrodynamic interaction between fine particles or between fine particles and the granular beds, which can be interpreted as a kind of hydrodynamic diffusion. Hydrodynamic diffusion was originally focused during the sedimentation of a fine particle assemblage in liquid without a granular bed (Nicolai et al., 1995; Guazzelli and Hinch, 2011). One of the major features of hydrodynamic diffusion has been known to be its anisotropy. It has been reported that the particles hydrodynamically diffuse more in the traveling direction than in the lateral directions. As shown in Fig. 4, even in the presence of a static granular bed, the fine particles spread more in the traveling direction than in the lateral direction.

Hydrodynamic diffusion is caused by the fluid-mediated interactions that alters the velocity of each particle. That is, the velocity difference among the particles, caused by the hydrodynamic interaction, leads to spreading. We investigated the velocity difference by calculating the standard deviation of the particle velocity during the permeation. In the present study, the position and velocity of the fine particle was separated into two components, i.e., in the traveling direction (z-direction) and in the perpendicular direction (on the $x-y$ plane). The standard deviation σ_z and σ_{xy} was calculated by traveling (z) and lateral (on the $x-y$ plane) components of the velocity vector of 40 fine particles and their ensemble average at each time, respectively. Both results were normalized by time and ensemble average $\langle \bar{U} \rangle$, where U indicates the magnitude of the velocity vector including all (x, y, and z) components.

Figure 5 shows the normalized standard deviation for the same conditions as Fig. 4 (ϕ_{in} = 2%, 7% and 12%). Because 15 trials were conducted in the present study by changing the initial position of fine particles and the arrangement of granular particles, the results and the error bars in Fig. 5 represent the average and the standard deviation of all trials, respectively. It is indicated that the larger the volume fraction of the granular bed, the larger the normalized standard deviation. This is because the hydrodynamics interaction between particles and granular bed is greater when the volume fraction is larger. Comparing z direction and lateral direction, σ_z is several times larger than σ_{xy}, indicating the anisotropy of velocity difference. This is consistent with the observation in Fig. 4, where the particles appear to be more spread out in the traveling (z) direction.

In order to quantitatively express the spread of fine particles, the dispersion of fine particle positions at each time was calculated. The dispersions in the traveling and lateral directions were respectively obtained by the following equations,

$$S^2(t_{01}) = \frac{1}{N-1}\sum_{i=1}^{N}(z_i - z_G)^2 \tag{7}$$

$$S^2(t_{01}) = \frac{1}{N-1}\sum_{i=1}^{N} {r_{Gi}}^2 \tag{8}$$

where N is the number of fine particles, z_i is the z-coordinate of fine particle i, and r_{Gi} is the distance between fine particle i and the mean position of all fine particles when projected on the x —y plane.

Figure 6 shows the temporal change in the dispersion of fine particle assemblage. Here, the dispersion is expressed as a difference from the dispersion $S^2(0)$ at the initial condition. The plots represent the average values of 15-times trials and the error bars represent the standard deviation. From Fig. 6, the dispersion tended to increase with the permeation time in both the traveling and lateral directions. On the other hand, when focusing on the slope of the increase, it tended to become larger with time in the traveling direction, and it increased at almost constant rate in the lateral direction. Note that in Fig.6, the range of the vertical scales are greatly different between (a) in the traveling direction and (b) in the lateral direction. Therefore, it was observed that the dispersion of the fine particle assemblage spread more in the traveling direction than that in the lateral direction. Although there is a difference in the presence or absence of a granular bed, the anisotropy of hydrodynamic diffusion is consistent with the predictions from Figs. 4 and 5, and also the literature (Nicolai et al., 1995; Guazzelli and Hinch, 2011).

Comparing the conditions with different volume fraction of stationary granular beds, it was found that, in the range of the present calculation conditions, the larger the volume fraction was, the larger the dispersion of the end time in the traveling direction became. This means that the denser the stationary granular bed is, the more the

assemblage of fine particles spreads. This is presumably related to the larger velocity difference among fine particles in the denser granular bed as shown in Fig. 5.

In the lateral direction, the dispersion tended to increase with decreasing particle bed volume fraction on average, although there were some variations depending on the trial as indicated by the long error bars. The velocity difference among particles shown in Fig. 5 is larger in denser granular bed, because the particles moves more while avoiding the stationary particles. At the same time, however, the particles less spread in the denser condition as shown in Fig. 6. This suggests that the particles do not simply diffuse laterally but weave through denser granular bed. In consequence, the particles which are less hindered by the granular bed with small volume fraction move freely, leading to larger lateral dispersion.

In this analysis, the time when the first fine particle went out of the granular bed region was set to the 'end time' and therefore, the time at which t_{01}=1 was not equal under each condition (c.f. Table 1) because the permeation resistance increased as the volume fraction increased. Since the larger the volume fraction was, the longer the permeation time was, the assemblage of fine particles was considered to spread taking more time. The index of spreadability, which is not affected by the difference in permeation time, will be discussed in section 3.3.

3.2 Behavior of fine particle assemblage through nonuniform bed

Figure 7 shows an example of the calculation results of fine particle assemblage behavior moving in a nonuniform granular bed. The volume fraction of the outer dense region was fixed at ϕ_{out} = 12%, and the volume fraction of the inner sparse region ϕ_{in} was set as various conditions. In the figure, the particle bed is translucent to make it easy to understand the particle position. Like in the uniform particle bed, fine particles

did not collide with each other, but passed through the static bed while changing their relative positions by hydrodynamic interactions. At the permeation end time, it was observed that the spread was larger under the condition of smaller ϕ_{in}. From these results, it is considered that the existence of sparse regions in the granular bed influenced the behavior of fine particle assemblages permeating through the bed.

As in Fig. 5, the standard deviations of the velocity of fine particles are shown in Fig. 8. Here, σ_z and σ_{xy} are normalized by the time and ensemble average of particles velocity through uniform granular bed with ϕ_{uni} = 12 % (same as the outer volume fraction ϕ_{out} of the nonuniform beds). From Fig. 8(a), the velocity differences in the traveling direction are larger for the granular beds of which the sparse region has smaller volume fraction. The normalized standard deviation in the lateral direction is almost the same for all conditions presented in Fig. 8(b), indicating that the lateral velocity differences do not depend on the volume fractions of sparse region.

In order to confirm the effect of the volume fraction in the sparse region on the behavior of fine particle assemblages, the temporal variation of fine particles located in the sparse region was investigated. The results are shown in Fig. 9. In this figure, samples 1~10 represent the results for the 10-times trials where the calculation was conducted by changing the random arrangement of stationary granular beds and the initial position of fine particles at each condition. From Fig. 9, it was found that under the uniform condition (c) $\phi_{in} = \phi_{out}$, the number of fine particles scarcely changed from the initial number. On the other hand, in the nonuniform conditions, (a) and (b), fine particles in the sparse region increased with time. At the permeation end time, about 60-75% for (a) and 45-60% for (b) of all fine particles was in the sparse region. From these results, it was found that when a granular bed has a nonuniform structure, fine particles gradually move from the dense region to the sparse region. We expected the standard

deviation of the lateral velocity to be larger in the condition of ϕ_{in} = 2% with more movement into the sparse region than that in the ϕ_{in} = 7% condition, but this is not the case in Fig. 8(b). This could be because many particles moved toward the central sparse region in the same way, which does not lead to change in velocity difference.

Figure 10 shows the distribution of fine particles in the granular bed at the end of permeation. The fine particles in sparse and dense regions were represented in red and black, respectively. Samples 1 to 10 are the same as those in Fig. 9. In Fig. 10, the z direction was separated into layers with the thickness of $10a_s$, and the ratio of fine particles in the sparse region (the number of fine particles in the sparse region of each layer, divided by the total number of fine particles in the same layer) was obtained. From Fig. 9, it was found that the ratio of fine particles in the sparse region increased with the decrease in the volume fraction in the sparse region. These results are the same as that observed in Fig. 9. In addition, it was also found that the ratio increased as the value of z approached z = 0. This is due to the fact that when fine particles exist in a sparse region, they move faster because they are less hindered by the granular beds.

Figure 11 shows the temporal changes in the dispersion of the positions for fine particle assemblages permeating a nonuniform granular bed. As well as Fig. 6, the results are shown in the form of a difference from the dispersion at the initial state. For z-direction in Fig. 11(a), the dispersion of fine particles increased with time as in the case of a uniform granular bed. In particular, the amount of dispersion increase became larger with decreasing volume fraction ϕ_{in} in the sparse region, and spread much larger than in the case of a uniform particle bed. From Figs. 9 and 10, it can be said that the smaller the ϕ_{in} was, the more the fine particles moved to the sparse region with small permeation resistance. In the dense region, the velocity of fine particles became smaller because particle motion is frequently hindered by the granular beds. It is considered that

a velocity difference between fine particles permeating through the sparse and dense regions was generated, so that the particles spread more widely. This is in agreement with Fig. 8(a).

For the lateral direction in Fig. 11(b), some conditions where the dispersion decreased with time were found. The fine particle assemblages spread with time, under the uniform condition of $\phi_{in} = 12\%$, and the dispersion scarcely changed for $\phi_{in} = 5\%$ and $\phi_{in} = 7\%$. On the other hand, for $\phi_{in} = 0\%$ and $\phi_{in} = 2\%$, there was a phenomenon where fine particles congregated more than those at the initial state (negative diffusion). The tendency where fine particles congregated in the center sparse region of the granular bed can be seen also from the results in Fig. 10. From the present results, it was found that when the volume fraction of the dense region is constant, fine particles can be laterally dispersed or collected depending on the condition of the volume fraction of the sparse region. These findings are expected to be applied to separation and sorting processes of fine particles.

3.3 Evaluation of hydrodynamic diffusion

Based on the above results, we propose a hydrodynamic diffusive index corresponding to the "diffusion coefficient". From this novel index, the spreading behavior due to hydrodynamic effects is quantitatively evaluated.

In the previous sections, the hydrodynamic diffusion of fine particle assemblage passing through uniform or nonuniform granular beds was quantitatively summarized. However, as mentioned in section 3.1, the time required for the permeation of the assemblage depends on the volume fraction of the granular beds. Table 1 shows the average permeation time under each condition. When the volume fraction of the granular bed was large, the permeation time was also long; therefore, it was confirmed

that the permeation end time described in the previous sections differed greatly depending on the conditions. Considering the difference in permeation time, an index that can quantitatively evaluate the spread per unit time was defined as follows,

$$D_{\mathrm{h}} = \frac{S^2(1) - S^2(0)}{t_{\mathrm{p}}} \tag{9}$$

where $S^2(0)$ and $S^2(1)$ are the dispersion of fine particle positions at the start and end times, respectively, and t_{p} is the time required for the permeation. The calculations of D_{h} by Eq. 9 were performed separately for the traveling (z) direction and lateral direction. The results of Eq. 9 using S^2 from Eq. 7 and Eq. 8 was called D_{h} in the traveling direction and lateral direction, respectively. By using this index, the spreadability is expressed from the viewpoint of how much the dispersion increases per unit time.

Figure 12 shows the relationship between D_{h} and the volume fraction ϕ_{uni} of uniform granular bed. From Fig. 12, it was found that in z-direction, there was no clear relationship between the particle bed volume fraction and D_{h}. In the previous research, hydrodynamic diffusion coefficient of fine particle assemblages in a liquid (without a granular bed) was obtained by velocity correlation (Nicolai et al., 1995), and it has been shown that there is a very distinctive relationship between the volume fraction of fine particle assemblages and hydrodynamic diffusion coefficient. In this study, the tendency as observed in the previous studies could not be observed due to the difference in the evaluation method of diffusion and the existence of a granular bed. In the range of this analysis, the volume fraction of the uniform bed had no significant effect on the spread of fine particles in the traveling direction per unit time.

In the lateral direction, it was found that the spread per unit time was remarkably large when the volume fraction in the sparse region was small, although the variation among the trials was large, especially in the small ϕ_{in} condition. It was also found that

the effect of the volume fraction became smaller when the granular bed was close to the uniform one. Since the granular bed with a smaller volume fraction did not interfere with the particle movement, it is considered that the particles moved freely in the lateral direction due to hydrodynamic interaction.

Figure 13 shows the relationship between D_h and the volume fraction in the sparse region for a nonuniform granular bed. The black, red, and blue plots show the results for the volume fraction in the dense region ϕ_{out} = 7%, 10%, and 12%, respectively. From Fig. 13, it was clarified that in the z-direction, the smaller ϕ_{in} was, the larger D_h became, and when the difference in the sparse and dense region increased, the fine particles tended to spread. This was similar to the results in Fig. 11, that is, the velocity difference was generated among fine particles due to the difference in the permeation resistance between sparse and dense regions. The same tendency was observed under the different ϕ_{out} conditions. When comparing the results of the same ϕ_{in}, the spreadability became maximum under the condition of ϕ_{out} = 12% where the sparse-dense difference was the largest in the present analysis.

In the lateral direction, as shown in Fig. 11, there was a negative spreading condition. Under the condition of relatively large ϕ_{in}, the value of D_h was positive. Especially when ϕ_{out} was small, it was found that the fine particles tended to be spread more. This tendency was the same as that observed in Fig. 12(b). On the other hand, when the value of ϕ_{in} was small and the difference in the volume fraction became large, the fine particle assemblages showed a negative diffusion. It was found that ϕ_{in}, which is the boundary between positive and negative diffusion, shifted to the right side of the graph (direction of larger ϕ_{in}) with the increase in ϕ_{out}.

In summary, in the uniform granular bed, there was no significant difference in the velocity at which fine particle assemblages spread in the traveling direction

regardless of the volume fraction. In the lateral direction, the smaller the volume fraction was, the more the particles spreading was. For nonuniform granular beds, the smaller the volume fraction of the sparse region in the traveling direction was, the faster the particles spread. On the other hand, the particles do not spread easily in the lateral direction when the volume fraction of the sparse region is small. In addition, when the volume fraction of the sparse region was enough small, the fine particle assemblages showed negative lateral spreading. The relationship between the spread of fine particle assemblages and the nonuniform structure using D_h as an index is expected to be applied to various engineering processes, such as the design of granular beds for the purpose of separating and sorting fine particles.

4. Conclusions

The Stokesian dynamics method was applied to simulate the behavior of fine particle assemblages permeating through a granular bed with uniform and nonuniform structure. It was observed that the assemblages were moving complexly while avoiding granular bed, resulting in hydrodynamic diffusion with particles spreading in both the traveling and lateral directions. The hydrodynamic spreading behavior was evaluated using the index D_h, which means the amount of particles dispersion increases per unit time. It was found that there was no significant difference in the speed at which the particle assemblages spread in the traveling direction in the uniform bed, regardless of the difference in the volume fraction of the granular bed. Also, it was found that in the lateral direction, the smaller the volume fraction was, the more the particle spreading was. For nonuniform beds, the larger the difference in sparse-dense volume fraction was, the more the particles spread in the traveling direction. In the lateral direction, the fine particle assemblages showed both positive and negative lateral spreading depending on the volume fractions. The relationship between a nonuniform structure

and the spread of fine particle assemblages using D_h as an index is expected to be applied to various engineering processes, such as the design of particle beds for the purpose of separating and sorting fine particles. At the present time, the effects of the particle size with few orders of magnitude, the polydispersity, and the volume fraction of the moving particles have not considered yet. These would be our future work.

Acknowledgment

This research is supported by JSPS KAKENHI Grant Number JP19H02252.

The authors report there are no competing interests to declare.

References

Ando, T., and J. Skolnick. 2010. Crowding and hydrodynamic interactions likely dominate in vivo macromolecular motion. The Proceedings of the National Academy of Sciences 107(43):18457−18462.

Brady, J. F., and G. Bossis. 1988. Stokesian dynamics. Annual Review of Fluid Mechanics 20:111−157.

Brady, J. F., R. J. Phillips, J. C. Lester, and G. Bossis. 1988. Dynamic simulation of hydrodynamically interacting suspensions. Journal of Fluid Mechanics 195:257−280.

Crowley, J. M. 1971. Viscosity-induced instability of a one-dimensional lattice of falling spheres. Journal of Fluid Mechanics 45:151−159.

Davis, R. H. 1996. Hydrodynamic diffusion of suspended particles: a symposium. Journal of Fluid Mechanics 310:325−335.

Durlofsky, L., J. F. Brady, and G. Bossis. 1987. Dynamic simulation of hydrodynamically interacting particles. Journal of Fluid Mechanics 180:21−49.

Ganatos, P., R. Pfeffer, and S. Weinbaum. 1978. A numerical-solution technique for three-dimensional Stokes flows, with application to the motion of strongly interacting spheres in a plane. Journal of Fluid Mechanics 84:79−111.

Guazzelli, E., and J. Hinch. 2010. Fluctuations and Instability in Sedimentation. Annual Review of Fluid Mechanics 43:97−116.

Harada, S., and R. Otomo. 2009. Diffusive behavior of a thin particle layer in fluid by hydrodynamic interaction. Physical Review E 80: 066311.

Jeffrey, D. J., and Y. Onishi. 1984. Calculation of the resistance and mobility functions for two unequal rigid spheres in low-Reynolds-number flow. Journal of Fluid Mechanics 139:261−290.

Joseph, G. G., R. Zenit, M. L. Hunt, and A. M. Rosenwinkel. 2001. Particle-wall collisions in a viscous fluid. Journal of Fluid Mechanics 433:329−346.

Kim, S., and S. J. Karrila. 2005. Microhydrodynamics: Principles and selected applications. New York: Dover Publications, Inc.

Nicolai, H., B. Herzhaft, E. J. Hinch, L. Oger, and E. Guazzelli. 1995. Particle velocity fluctuations and hydrodynamic self-diffusion of sedimenting non-Brownian spheres. Physics of Fluids 7:12−23.

Nott, P. R., and J. F. Brady. 1994. Pressure-driven flow of suspensions: simulation and theory. Journal of Fluid Mechanics 275:157−199.

Otomo, R., and R. Kira. 2021. The effect of the layered internal structure of fibrous beds on the hydrodynamic diffusive behavior of microparticles. Micromachines 12: 1241.

Otomo, R., and K. Mori. 2021. Numerical analysis on motion of microparticles passing through straight and tortuous fibrous layers. Fluid Dynamics Research 53:025503.

Phillips, R. J., J. F. Brady, and G. Bossis. 1988. Hydrodynamic transport properties of hard-sphere dispersions. I. Suspensions of freely mobile particles. Physics of Fluids 31(12):3462−3472.

Singh, A., and P. R. Nott. 2000. Normal stresses and microstructure in bounded sheared suspensions via Stokesian Dynamics simulations. Journal of Fluid Mechanics 412:279−301.

Skaug, M. J., L. Wang, Y. Ding, and D. K. Schwartz. 2015. Hindered nanoparticle diffusion and void accessibility in a three-dimensional porous media. ACS Nano 9(2):2148−2156.

Table 1. Average permeation time of fine particle assemblage. (a) Uniform bed (b) Nonuniform bed (ϕ_{out} = 12%).

Figure 1. Calculation domain and initial arrangement. (a) Uniform granular bed, (b) Nonuniform granular bed.

Figure 2. Examples of initial arrangements with various volume fraction. (a) Uniform granular bed, (b) Nonuniform granular bed (ϕ_{out} = 12%).

Figure 3. Relation between repulsive force and surface distance of two particles.

Figure 4. Fine particles behavior through uniform granular beds.

Figure 5. Time change of normalized standard deviation of particles velocity through uniform granular bed. (a) traveling (z) direction, (b) lateral direction.

Figure 6. Time change of variance of fine particles position through uniform bed. (a) traveling (z) direction, (b) lateral direction.

Figure 7. Fine particles behavior through nonuniform granular beds (ϕ_{out} = 12%).

Figure 8. Time change of normalized standard deviation of particles velocity through nonuniform granular bed. (a) traveling (z) direction, (b) lateral direction.

Figure 9. Time change in the number of particles in sparse region.

Figure 10. Spatial distribution of fine particles and ratio of particles in dilute region to all particles at t_{01} = 1.0.

Figure 11. Time change of variance of fine particles position through nonuniform bed (ϕ_{out} = 12%). (a) traveling (z) direction, (b) lateral direction.

Figure 12. Relation between volume fraction of uniform granular bed ϕ_{uni} and hydrodynamic diffusion index D_h. (a) traveling (z) direction, (b) lateral direction.

Figure 13. Relation between volume fraction of nonuniform granular bed ϕ_{in}, ϕ_{out} and hydrodynamic diffusion index D_h. (a) traveling (z) direction, (b) lateral direction.

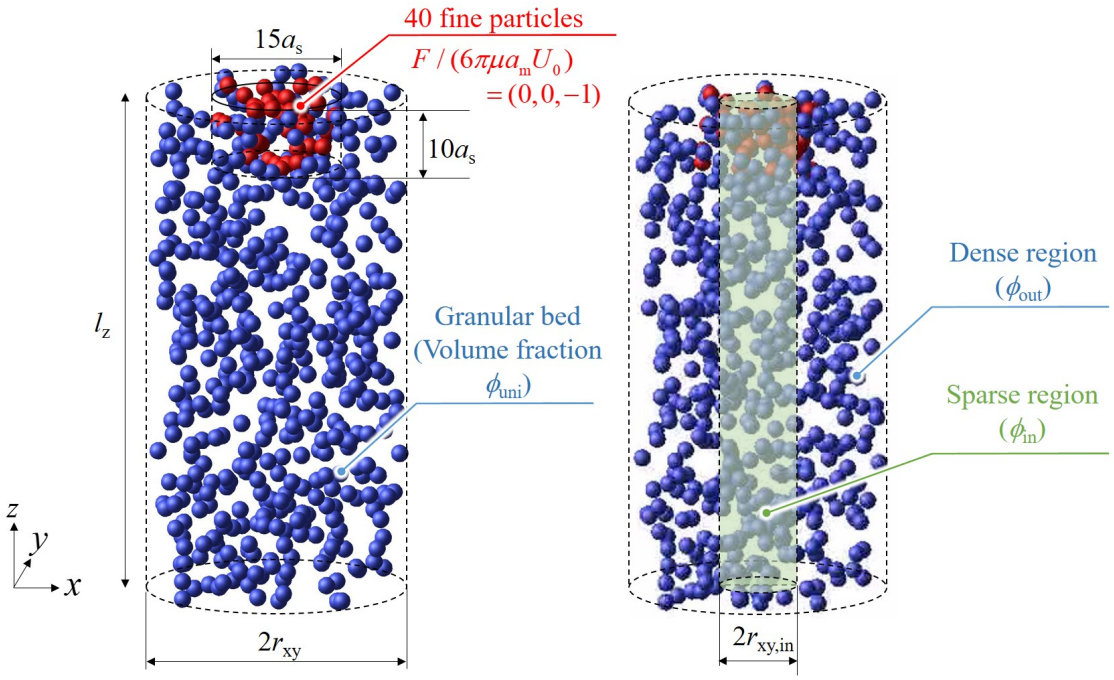
40 fine particles
$F/(6\pi\mu a_m U_0) = (0,0,-1)$
$15a_s$
$10a_s$
l_z
Granular bed
(Volume fraction
ϕ_{uni})
Dense region
(ϕ_{out})
Sparse region
(ϕ_{in})
z
y
x
$2r_{xy}$
$2r_{xy,in}$

Fig. 1

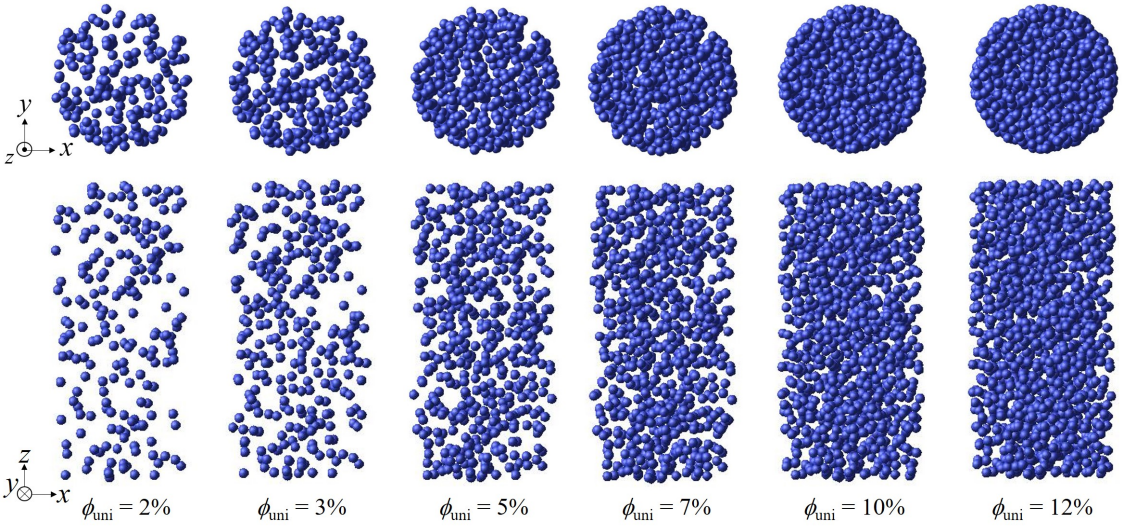
y
x
z
z
y
x
ϕ_{uni} = 2%
ϕ_{uni} = 3%
ϕ_{uni} = 5%
ϕ_{uni} = 7%
ϕ_{uni} = 10%
ϕ_{uni} = 12%

(a)

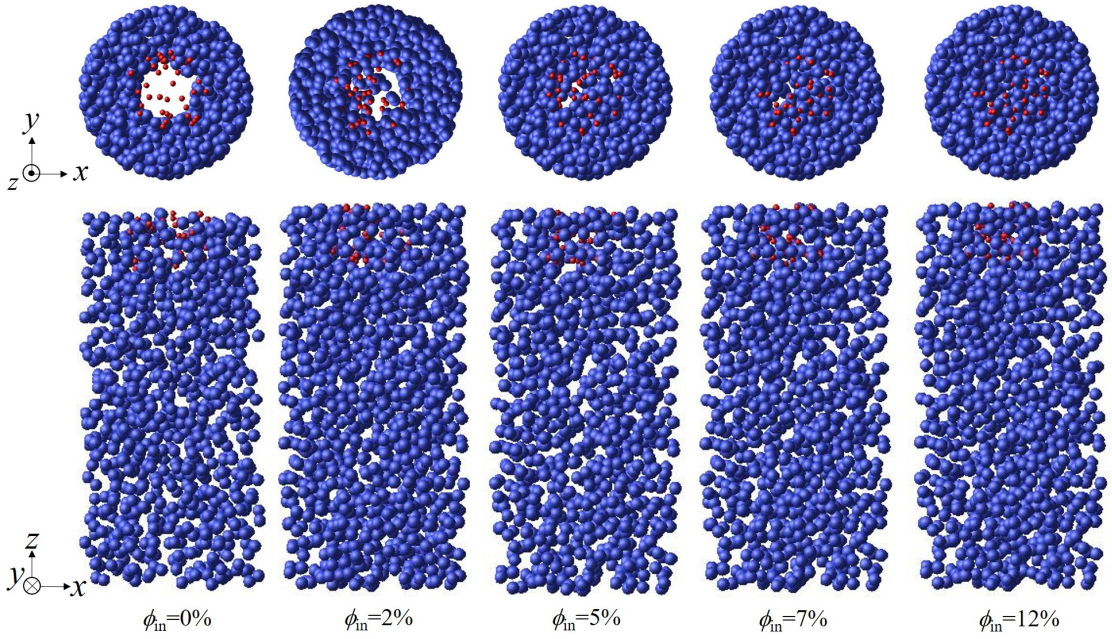
y
x
z
z
y
x
ϕ_{in}=0%
ϕ_{in}=2%
ϕ_{in}=5%
ϕ_{in}=7%
ϕ_{in}=12%

(b)

Fig. 2

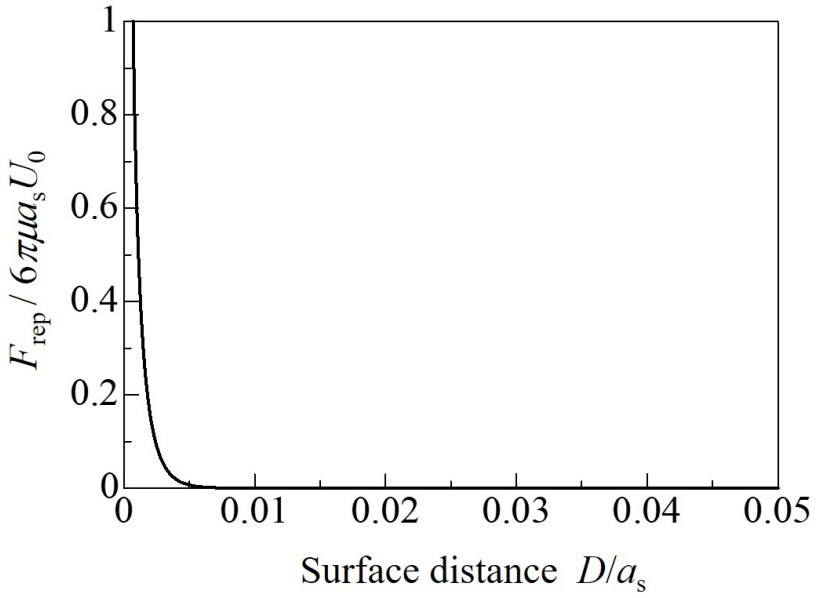
1
0.8
0.6
0.4
0.2
0
0
0.01
0.02
0.03
0.04
0.05
$F_{rep} / 6\pi\mu a_s U_0$
Surface distance D/a_s

Fig. 3

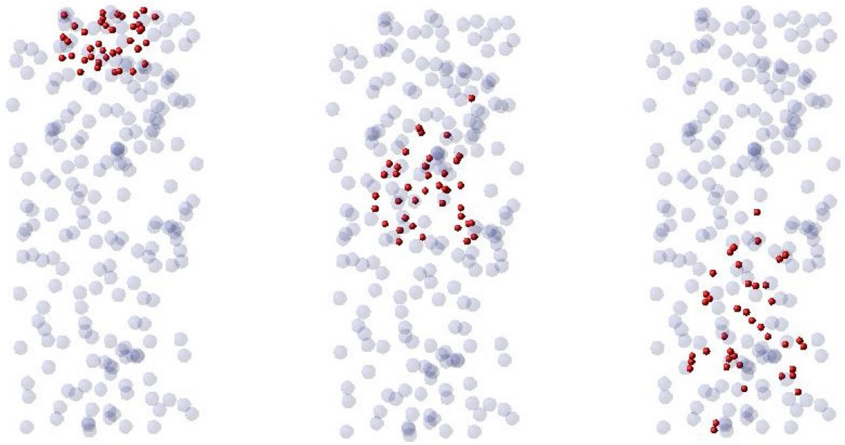

t_{01}=0.0 t_{01}=0.5 t_{01}=1.0

(a) ϕ_{uni} = 2%

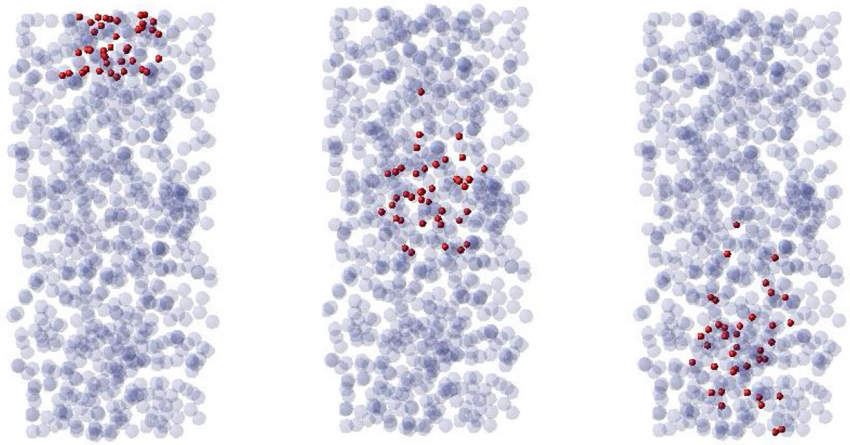

t_{01}=0.0 t_{01}=0.5 t_{01}=1.0

(b) ϕ_{uni} = 7%

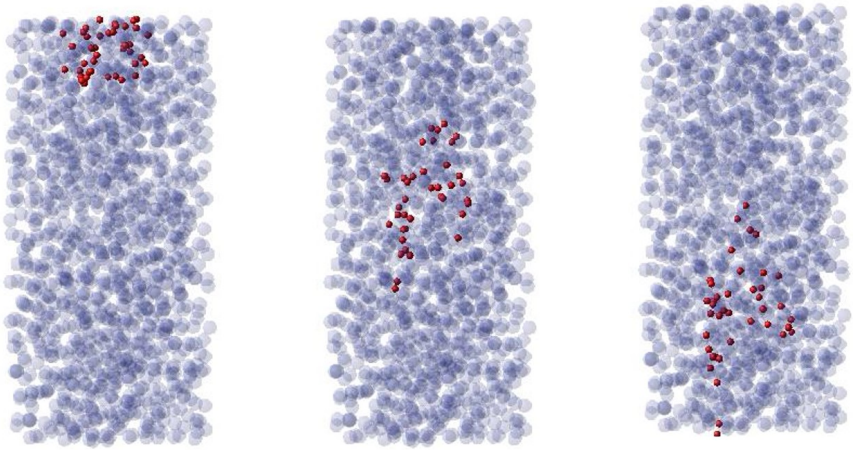

t_{01}=0.0 t_{01}=0.5 t_{01}=1.0

(c) ϕ_{uni} = 12%

Fig. 4

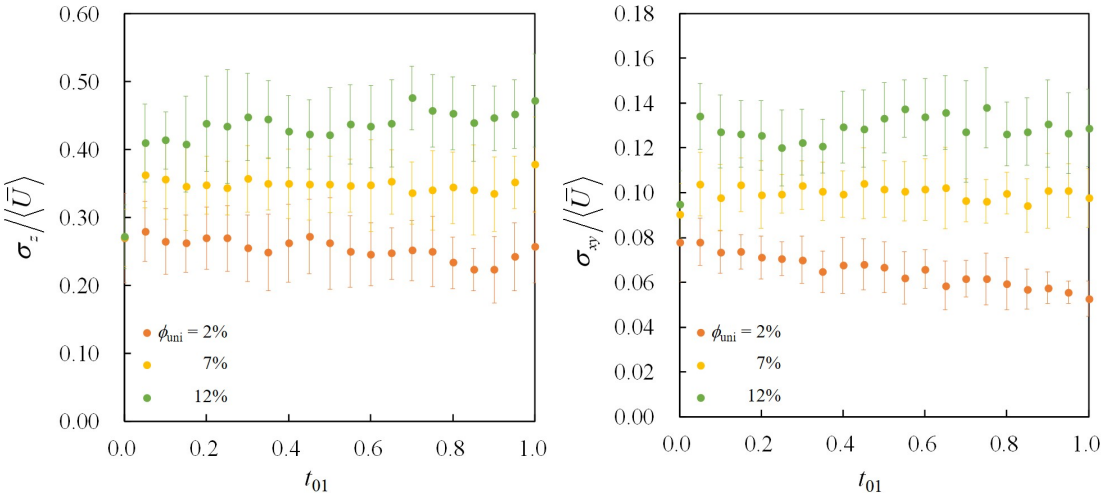
0.60
0.50
0.40
0.30
0.20
0.10
0.00
$\sigma_z/\langle\bar{U}\rangle$
ϕ_{uni} = 2%
7%
12%
0.0
0.2
0.4
0.6
0.8
1.0
t_{01}
0.18
0.16
0.14
0.12
0.10
0.08
0.06
0.04
0.02
0.00
$\sigma_{xy}/\langle\bar{U}\rangle$
ϕ_{uni} = 2%
7%
12%
0.0
0.2
0.4
0.6
0.8
1.0
t_{01}

Fig. 5

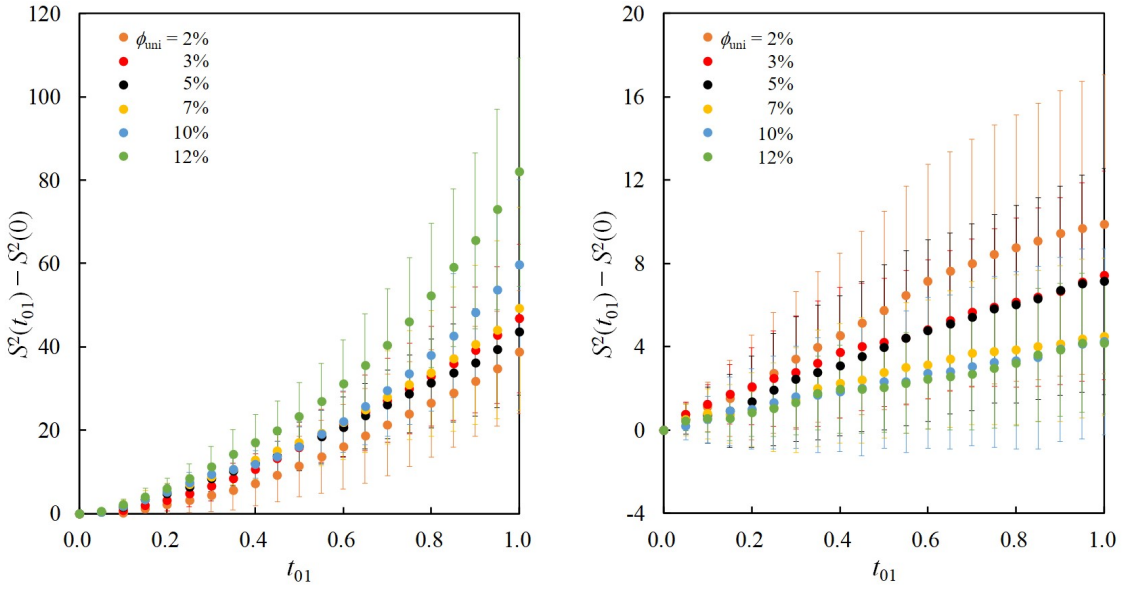
120
100
80
60
40
20
0
$S^2(t_{01}) - S^2(0)$
ϕ_{uni} = 2%
3%
5%
7%
10%
12%
0.0
0.2
0.4
0.6
0.8
1.0
t_{01}
20
16
12
8
4
0
-4
$S^2(t_{01}) - S^2(0)$
ϕ_{uni} = 2%
3%
5%
7%
10%
12%
0.0
0.2
0.4
0.6
0.8
1.0
t_{01}

Fig. 6

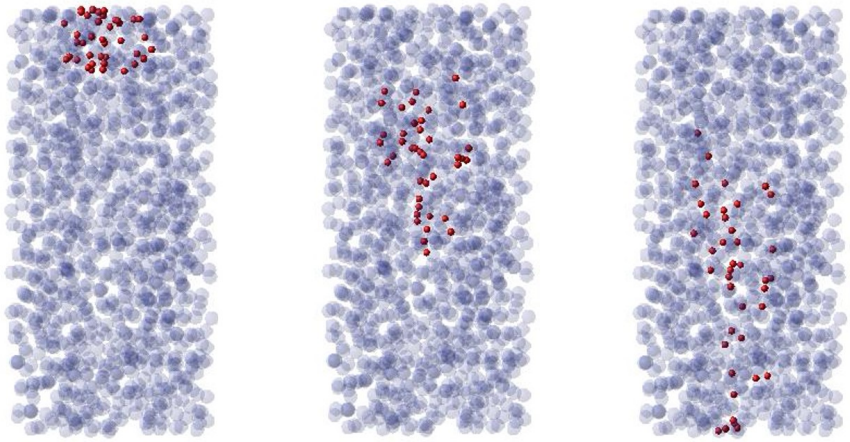

t_{01}=0.0 t_{01}=0.5 t_{01}=1.0

(a) ϕ_{in}= 2%

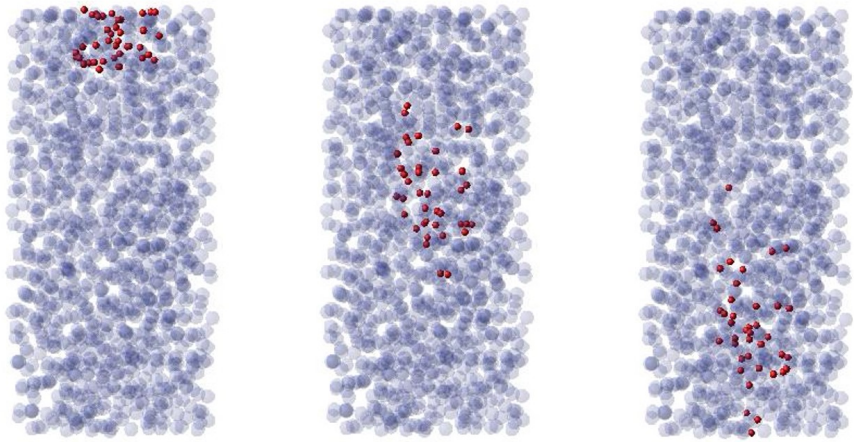

t_{01}=0.0 t_{01}=0.5 t_{01}=1.0

(b) ϕ_{in}= 7%

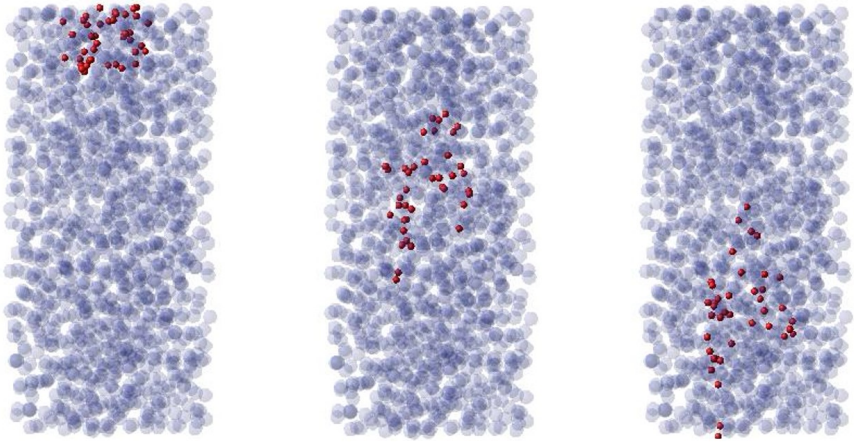

t_{01}=0.0 t_{01}=0.5 t_{01}=1.0

(c) ϕ_{in}= 12%

Fig. 7

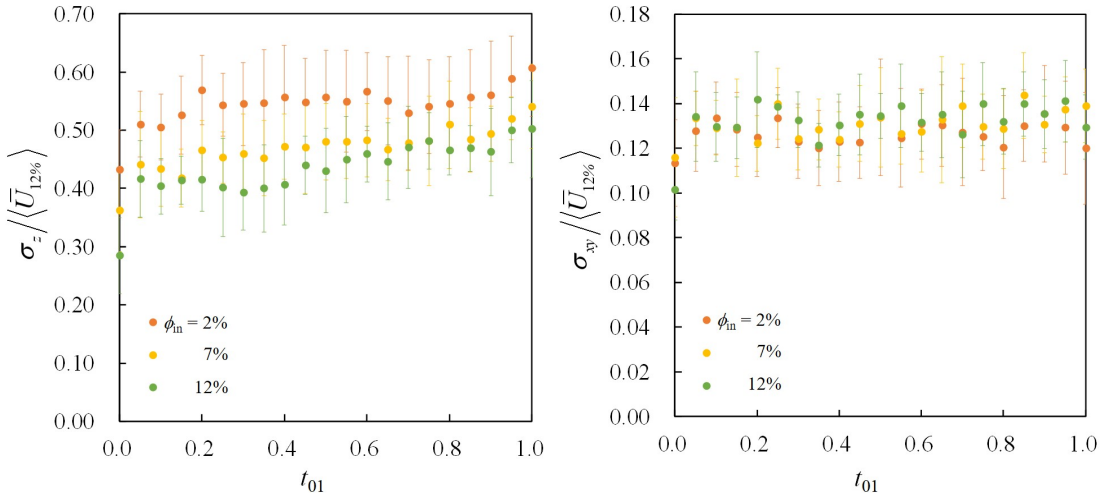

Fig. 8

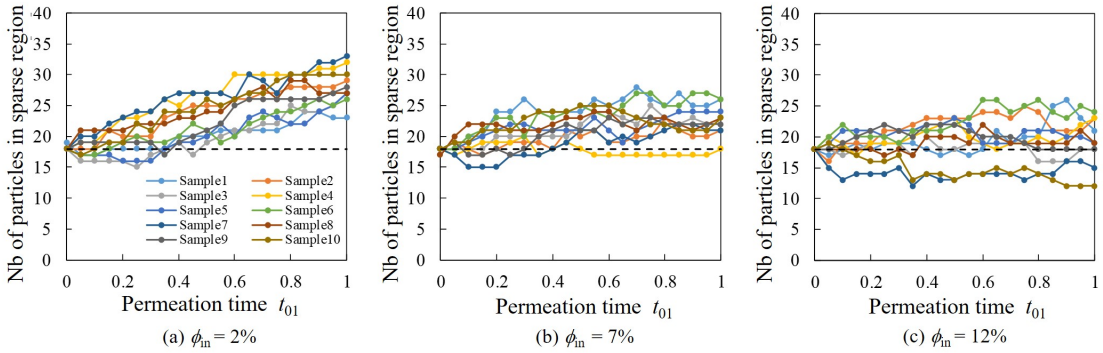

(a) ϕ_{in} = 2% (b) ϕ_{in} = 7% (c) ϕ_{in} = 12%

Fig. 9

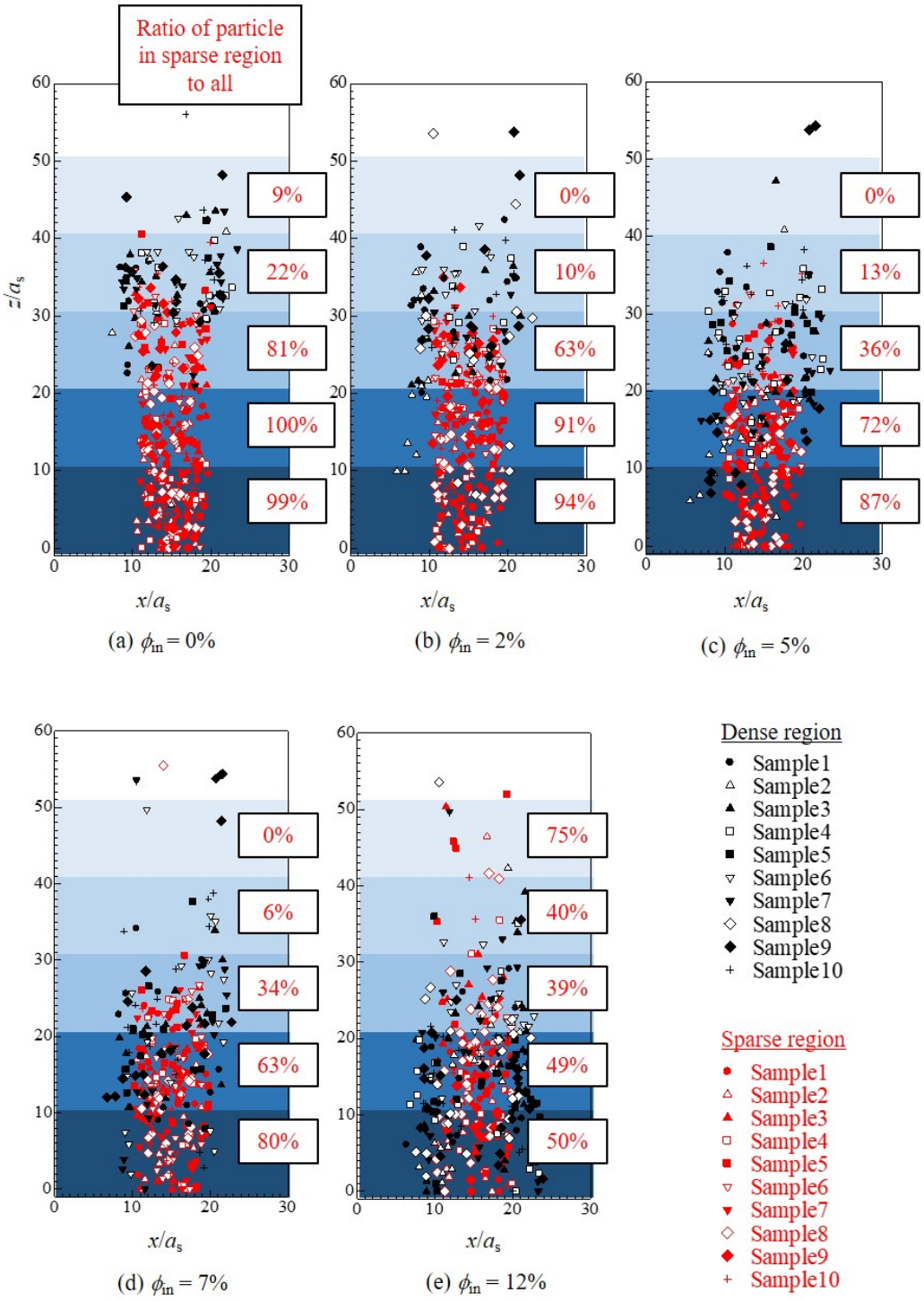
Ratio of particle in sparse region to all
9%
22%
81%
100%
99%
0%
10%
63%
91%
94%
0%
13%
36%
72%
87%
0%
6%
34%
63%
80%
75%
40%
39%
49%
50%
z/a_s
x/a_s
(a) $\phi_{in} = 0\%$
(b) $\phi_{in} = 2\%$
(c) $\phi_{in} = 5\%$
(d) $\phi_{in} = 7\%$
(e) $\phi_{in} = 12\%$
Dense region
Sample1
Sample2
Sample3
Sample4
Sample5
Sample6
Sample7
Sample8
Sample9
Sample10
Sparse region
Sample1
Sample2
Sample3
Sample4
Sample5
Sample6
Sample7
Sample8
Sample9
Sample10

Fig. 10

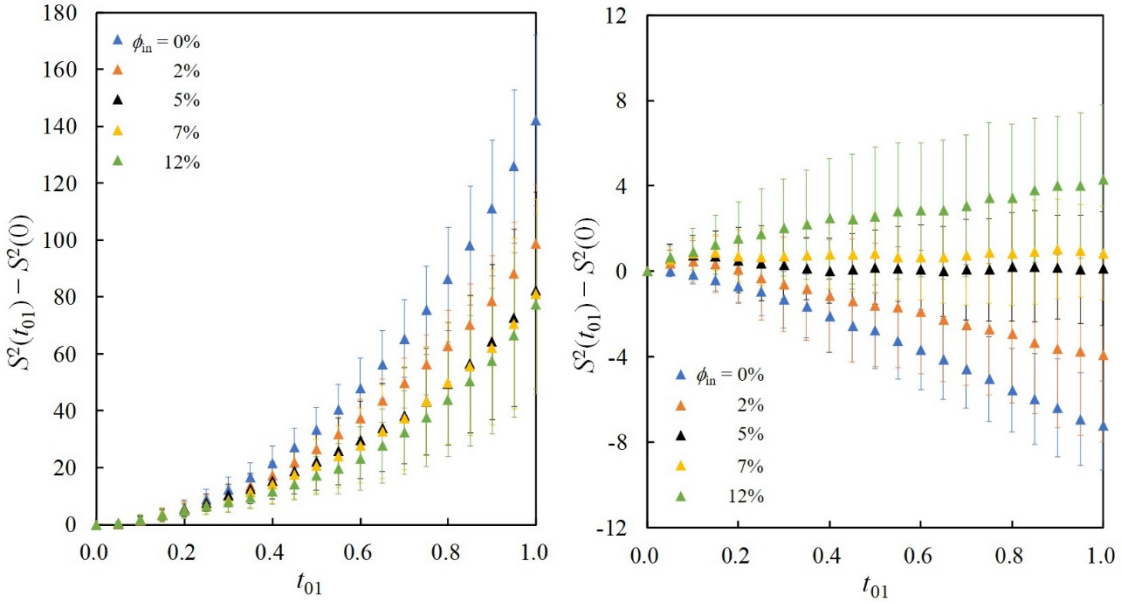

Fig. 11

Table 1

(a)

Volume fraction ϕ_{uni} [%]	Average permeation time $t_{ave}/(a_s/U_0)$
2	35.8
3	41.3
5	46.9
7	57.4
10	68.8
12	72.8

(b)

Volume fraction in sparse region ϕ_{in} [%]	Average permeation time $t_{ave}/(a_s/U_0)$
0	38.3
2	47.9
5	56.3
7	61.3
12	69.2

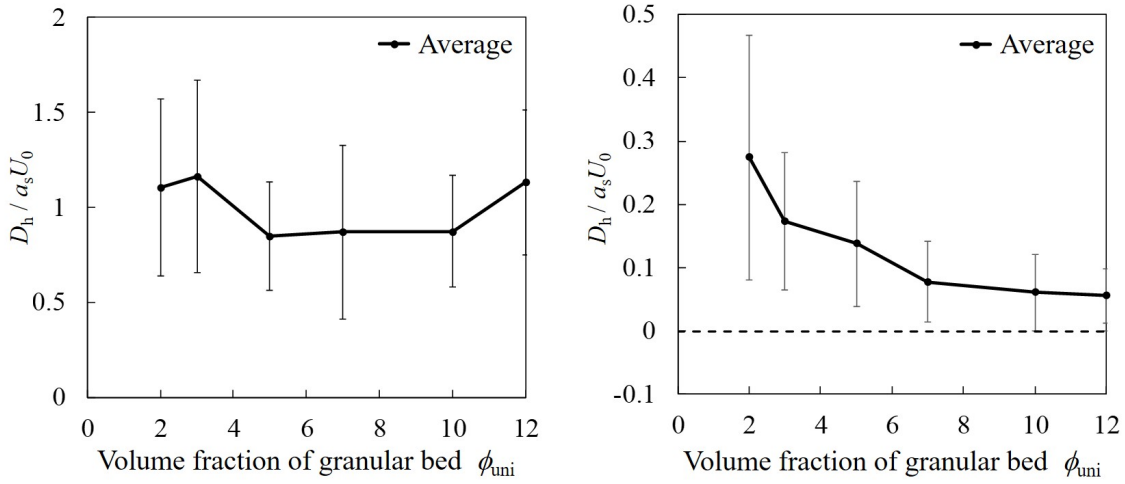
Average
$D_h / a_s U_0$
Volume fraction of granular bed ϕ_{uni}
Average
$D_h / a_s U_0$
Volume fraction of granular bed ϕ_{uni}

Fig. 12

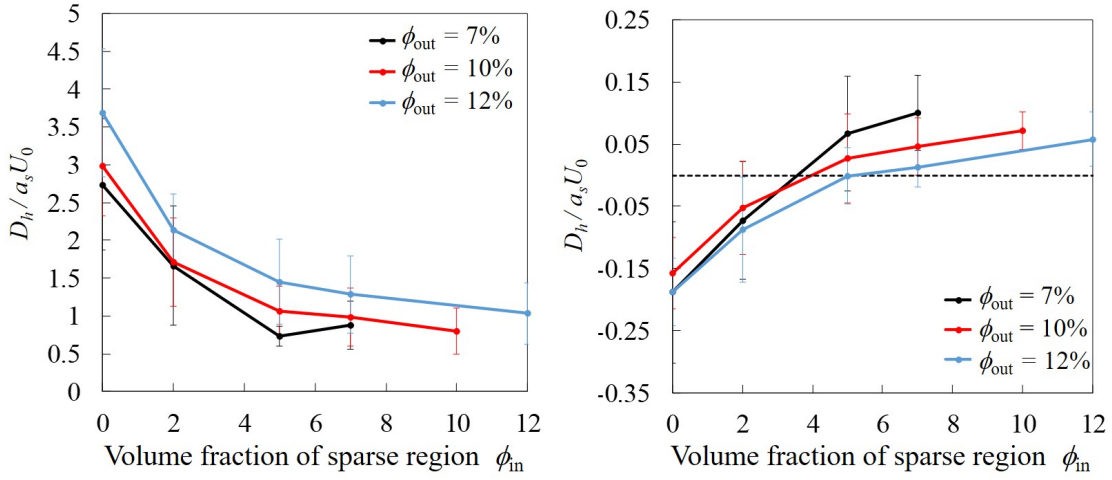
ϕ_{out} = 7%
ϕ_{out} = 10%
ϕ_{out} = 12%
$D_h / a_s U_0$
Volume fraction of sparse region ϕ_{in}
ϕ_{out} = 7%
ϕ_{out} = 10%
ϕ_{out} = 12%
$D_h / a_s U_0$
Volume fraction of sparse region ϕ_{in}

Fig. 13